C.P. No. 92
(13,787)
A R C Technical Report

MINISTRY OF SUPPLY

AERONAUTICAL RESEARCH COUNCIL

CURRENT PAPERS

Tests in the Compressed Air Tunnel on Two Aerofoil Sections having a Large Scale Effect on C_{Lmax} at a Critical Reynolds Number

By

C. Salter, M. A., Miss H.M. Lee, B.Sc., and Miss R. C. Owen,
of the Aerodynamics Division, N.P.L.

LONDON HER MAJESTY'S STATIONERY OFFICE

1952

FOUR SHILLINGS NET

C.P. No. 92.

Tests in the Compressed Air Tunnel on Two Aerofoil Sections having a Large Scale Effect on $C_L$max at a Critical Reynolds Number.

- By -
C. Salter, M.A., Miss H. M. Lee, B.Sc. and Miss R. C. Owen
of the Aerodynamics Division, N.P.L.

16th February, 1951

Summary

The report gives results of tests on two "constant velocity" aerofoil sections, 9% and 11% thick respectively, and of aspect ratio 6, over a range of R of 0.3×10^6 to 7.5×10^6.

In both cases $C_L$max. is 0.8 at low Reynolds numbers but rises very sharply between $R = 1 \times 10^6$ and 2×10^6 to 1.3 or 1.4, reaching a value of nearly 1.5 at $R = 4 \times 10^6$. The stall is very sharp at Reynolds numbers above the critical value and the slopes of the $C_L - \alpha$ curves are not very different in the two cases over most of the range. Above $C_L = 0.5$ however, the slope for the thin wing appears to increase somewhat while the tendency for the thicker wing is in the other direction.

C_{D_0}min. is lower for the 11% than for the 9% section except at low Reynolds numbers (where the reverse is found) and at high Reynolds numbers (where the values are nearly equal).

$\frac{dC_m}{dC_L}$ at low lift coefficients is generally somewhat higher for the 11%. An appendix gives the results of tufting experiments.

Introduction

These wing sections were examined as a result of preliminary tests, on an aircraft model, which made it desirable to check the profile characteristics. The thickness/chord ratio in the original design varied from 12% near the root to 11% at the tip but the outer parts of the wing were later modified to a 9% thick section.

Derivation of Profiles

The basic wing sections were designed by the method given by Thwaites in Refs. 1 and 2. The specification was for constant velocity on the upper surface up to 0.40 chord (11% t/c) and 0.35 chord (9% t/c) at $C_L = 0.26$ and 0.18 respectively. This was associated with a constant loading type camber line (Ref. 3) which gave constant loading on the 11% wing up to 0.60 chord decreasing linearly to zero at the trailing edge at a $C_L$opt. of 0.13. The same camber line was used for the 9% section. The rear portions of both sections were slightly cusped. The maximum thicknesses of the sections were located at 0.43c (11% t/c) and 0.34c (9% t/c).

/The

Published with permission of the Director, National Physical Laboratory.

The upper and lower surface ordinates are recorded in Table I while the profiles are sketched in Fig.1. The ordinates were checked by plotting mean slopes at different parts of the outline against distance from the leading edge. Some obvious small errors were found and the figures given in the table therefore differ slightly from those supplied by the firm.

Wing Models and Supports

The 9% wing was made of steel and the 11% of hiduminium (R.R.56). Both were rectangular in plan form. The nominal chord was 8 inches and the span 4 ft. but the chord of the 9% wing, was actually 7.94 in.. giving an aspect ratio of 6.045 instead of 6 while the 11% model was slightly bent in the direction of the span. As a result of this curvature the end chords of the 11% wing were nearly 0.08 in. below the centre chord (wing right way up).

The thicker wing was mounted (upside down) on the standard end-pin and tail supports. The 9% wing however, was too thin to be held in this way and was therefore suspended from streamlined rods at points $24\frac{3}{4}$ in. apart and 1.6 in. from the leading edge. The adjustable rear support was located near the centre of the trailing edge in each case.

Range of Tests

The tests included measurements of lift, drag and pitching moment ranging from negative values of C_L to the stalled region. Reynolds numbers varied from 0.3×10^6 to 7.2×10^6 (9% wing) and 7.6×10^6 (11% wing).

Tables and Figures

A summary of results is given in Table II and details of the observations in Tables III and IV. The summary is illustrated in Fig.II and typical curves of C_L against α and C_m against C_L are drawn in Fig.3.

In addition to the normal tunnel corrections for drag and incidence, the aspect ratio corrections that have been used in the calculation of α_o are

$$- 3.52\ C_L \text{ degrees } (9\%) \quad \text{and} \quad - 3.55\ C_L \text{ degrees } (11\%)$$

while the induced drag coefficient has been estimated from the expressions

$$0.055\ C_L^2\ (9\%) \quad \text{and} \quad 0.0555\ C_L^2\ (11\%).$$

Results

Lift.

The differences in $C_L$max. are small, and except at very low Reynolds numbers, the stall is very sharp in both cases (Fig.3). With R approaching 1.5×10^6 the maximum lift coefficient begins to rise steeply. At low values of R, $C_L$max. is 0.8 and at high values nearly 1.5 (Fig.2).

The slope of the lift curve is generally much the same in each case. For the 9% section the values given in Table II and plotted in Fig.2 cover a range of C_L of -0.12 to +0.5. There appears generally to be a slight increase at greater angles of incidence. The values quoted for the 11% section refer to C_L ranging from -0.1 to +0.35 up to R = 2×10^6 and -0.1 to +0.75 for R greater than this. In this case the slope decreases at higher angles of incidence.

As/

As mentioned in a previous paragraph, a_o has been calculated by the use of the Glauert "lifting line" formula. The slope of the C_L against α_o curve however, is appreciably different if the Bryant-Garner equation,

$$\frac{A}{a} = \frac{A}{a_o} + 0.34\,(1 + \tau) + 0.064\sqrt{\frac{a_o}{A}}\ ,$$

based on lifting surface theory is employed.

The calculated values for high Reynolds numbers are as follows:

	$a = \dfrac{dC_L}{d\alpha}$	$a_o = \dfrac{dC_L}{d\alpha_o}$ Glauert	$a_o = \dfrac{dC_L}{d\alpha_o}$ Bryant
9%	4.3	5.85	6.4
11%	4.4	6.04	6.6

At zero lift α is -0.6 degrees for the 9% wing and -0.9 degrees for the 11% wing, while at $\alpha = 0$, the values of C_L are approximately 0.045 and 0.065 respectively. The shift of the curve is illustrated in Fig.3.

Pitching Moment

The relation between C_m and C_L is also much the same in the two cases (Fig.3) but the value of $\dfrac{dC_m}{dC_L}$ at the lower lift coefficients is appreciably different (Table II and Fig.2). The slopes recorded cover the range of C_L from -0.12 to +0.35 or 0.4 (9% wing) and -0.1 to roughly +0.5 (11% wing).

Moments are given about the quarter chord line in each case.

Drag

C_{D_O} min. is lower for the 11% than for the 9% section except at low Reynolds numbers, where the reverse is found, and at the highest Reynolds number of $7\frac{1}{2} \times 10^6$, where the values are nearly equal and of magnitude approximately 0.007 (Table II and Fig.2).

The slope of the C_D against $C_L{}^2$ curves at low lift could only be measured in a few cases and then with uncertain accuracy. Sufficient measurements were however, available to show the usual relatively high values of slope at low Reynolds numbers tending to the Glauert value of 0.0555 at high values of R.

(Note on $C_L$max :- Allowing an increase of 5% for infinite aspect ratio, $C_L$max for the 11% wing fits well on the curves of Multhopp's analysis for cambered aerofoils (Ref. 4); for the 9% it is inclined to be rather high by roughly 0.1.)

References/

References

No.	Author	Title, etc.
1	B. Thwaites	A method of aerofoil design. Part I - Symmetrical aerofoils. R. & M. 2166. May, 1945.
2	B. Thwaites	A method of aerofoil design. Part II - Cambered aerofoils. R. & M. 2167. September, 1945.
3	E. J. Richards	A family of camber lines for low drag aerofoils giving an arbitrary pitching moment coefficient. A.R.C. 8277. (Unpublished).
4	H. Multhopp	On the maximum lift coefficient of aerofoil sections. A.R.C. 12,115. December, 1948.
5	D. D. Carrow	A note on the boundary layer and stalling characteristics of aerofoils. A.R.C. 13,424. (Unpublished). 5th October, 1950.
6	A. D. Young	A review of some stalling research. With an Appendix by H. B. Squire and A. D. Young. R. & M. 2609. February, 1942.

Table I

Ordinates of Aerofoil Sections

(Inches)

x ins.	Aerofoil Profile 11% t/c		Aerofoil Profile 9% t/c	
	y_u	y_l	y_u	y_l
0	L.E. Radius	0.088	L.E. Radius	0.084
0.04	0.082	0.075	0.083	0.075
0.06	0.098	0.088	0.099	0.089
0.10	0.122	0.106	0.123	0.108
0.20	0.164	0.137	0.162	0.134
0.40	0.226	0.180	0.216	0.169
0.60	0.274	0.212	0.258	0.195
0.80	0.314	0.238	0.292	0.215
1.20	0.377	0.278	0.345	0.244
1.60	0.426	0.307	0.385	0.264
2.00	0.463	0.329	0.412	0.278
2.40	0.491	0.344	0.429	0.284
2.80	0.509	0.354	0.437	0.282
3.20	0.520	0.359	0.434	0.273
3.60	0.522	0.358	0.423	0.258
4.00	0.515	0.350	0.405	0.239
4.40	0.497	0.337	0.379	0.218
4.80	0.470	0.318	0.346	0.194
5.20	0.433	0.293	0.308	0.168
5.60	0.385	0.262	0.264	0.141
6.00	0.327	0.224	0.218	0.114
6.40	0.261	0.179	0.171	0.088
6.80	0.189	0.128	0.125	0.064
7.20	0.117	0.078	0.081	0.042
7.40	0.084	0.055	0.062	0.032
7.60	0.053	0.035	0.041	0.023
7.80	0.026	0.018	0.023	0.015
7.90	0.015	0.011	0.014	0.010
8.00	0	0	0	0

	Aerofoil Profile 11% t/c	Aerofoil Profile 9% t/c
Span	4 ft.	4 ft.
Chord	0.662 ft.	0.667 ft.
A.R.	6.045	6.0
Wing Area	2.645 sq. ft.	2.667 sq. ft.
Max t/c at	0.43c	0.34c
$\frac{t_{0.05}}{c}$	0.051	0.048

Table II/

Table II

Summary of Results

$\frac{R}{10^6}$	log R	$C_L$max	Incidence at $C_L$max. (degrees)	C_{D_0}min.	$\frac{dC_L}{d\alpha}$ (α in radians)	$\frac{dC_m}{dC_L}$
9% Aerofoil						
0.287	5.46	0.805	12.0	0.0080	4.16	-
0.91	5.96	0.85	12.7	0.0066	4.225	0.017
1.51	6.18	0.995	12.6	0.0061	4.25	0.0096
2.20	6.34	1.385	18.85	0.0061	4.30	0.0095
2.98	6.475	1.435	19.45	0.0063	4.32	0.0098
3.26	6.515	1.47	20.0	-	-	-
4.05	6.61	1.475	20.15	0.0069	4.32	0.0102
5.76	6.76	1.475	20.15	0.0069	4.30	0.0103
7.19	6.855	1.43	19.4	0.0070	4.29	0.0097

$\frac{dC_L}{d\alpha}$ refers to range of C_L = -0.12 to +0.5

Slope generally shows slight increase at high values of C_L.

$\frac{dC_m}{dC_L}$ refers to range of C_L = -0.12 to +0.35 (R up to 4×10^6)
-0.12 to +0.4 (R over 4×10^6)

$\frac{R}{10^6}$	log R	$C_L$max	Incidence at $C_L$max. (degrees)	C_{D_0}min.	$\frac{dC_L}{d\alpha}$ (α in radians)	$\frac{dC_m}{dC_L}$
11% Aerofoil						
0.30	5.48	0.80	12.2	0.0106	3.98	0.041
0.65	5.81	0.815	12.5	0.0072	4.21	0.036
1.075	6.03	0.825	12.5	0.0050	4.24	0.0296
1.47	6.165	0.855	12.5	-	-	-
2.08	6.32	1.30	19.0	0.0046	4.30	0.0217
2.91	6.465	1.395	20.5	-	-	-
4.12	6.615	1.485	21.6	-	-	-
5.05	6.705	1.485	21.85	0.0061	4.27	0.0186
5.73	6.76	1.48	21.1	-	-	-
6.65	6.825	1.465	20.7	0.0068	4.42	0.017
7.64	6.885	1.455	20.25	0.0068	4.44	0.0144

$\frac{dC_L}{d\alpha}$ refers to range of C_L = -0.1 to +0.35 (R up to 2×10^6)
-0.1 to +0.75 (R over 2×10^6)

Slope decreases at higher values of C_L

$\frac{dC_m}{dC_L}$ refers to range of C_L = -0.1 to +0.5 roughly.

Table III/

<u>Table III</u>

<u>9% Wing</u>

P = 1.0 Atmos. V = 72.0 FPS			ρV^2 = 12.1 lb./sq.ft. R = 0.287 × 10^6			P = 4.3 Atmos. V = 53.2 FPS			ρV^2 = 27.9 lb./sq. ft. R = 0.91 × 10^6			P = 8.0 Atmos. V = 47.7 FPS			ρV^2 = 41.6 lb./sq. ft. R = 1.51 × 10^6		
α	C_L	C_D	C_{D_0}	C_m	α_0	α	C_L	C_D	C_{D_0}	C_m	α_0	α	C_L	C_D	C_{D_0}	C_m	α_0
-2.15	-0.096	0.0122	0.0117	-0.0274	-1.8	-2.15	-0.119	0.0109	0.0101	-0.0232	-1.75	-2.2	-0.121	0.0093	0.0085	-0.0219	-1.75
-0.85	-0.010	0.0091	0.0091	-0.0237	-0.8	-0.9	-0.023	0.0091	0.0091	-0.0218	-0.8	-0.9	-0.025	0.0080	0.0080	-0.0212	-0.8
+0.4	+0.074	0.0091	0.0088	-0.0194	+0.1	+0.35	+0.065	0.0077	0.0075	-0.0198	+0.1	+0.35	+0.068	0.0068	0.0066	-0.0201	+0.1
1.65	0.169	0.0100	0.0084	-0.0182	1.05	1.6	0.159	0.0082	0.0068	-0.0191	1.05	1.6	0.161	0.0075	0.0061	-0.0191	1.05
2.85	0.266	0.0120	0.0081	-0.0182	1.9	2.85	0.249	0.0101	0.0067	-0.0167	1.95	2.85	0.255	0.0101	0.0065	-0.0183	1.95
5.3	0.440	0.0269	0.0163	-0.0151	3.75	5.25	0.433	0.0192	0.0089	-0.0154	3.75	5.25	0.438	0.0188	0.0073	-0.0168	3.7
7.8	0.609	0.0353	0.0151	-0.0114	5.65	7.75	0.617	0.0318	0.0109	-0.0148	5.55	7.75	0.632	0.0310	0.0091	-0.0154	5.55
10.25	0.763	0.0652	0.0332	-0.0066	7.55	9.0	0.709	0.0394	0.0117	-0.0138	6.5	10.15	0.812	0.0475	0.0113	-0.0149	7.3
11.5	0.800	0.108	0.0727	-0.0261	8.7	10.15	0.793	0.0485	0.0139	-0.0128	7.35	11.4	0.906	0.0573	0.0122	-0.0148	8.2
12.8	0.790	0.153	0.119	-0.0626	10.0	11.45	0.826	0.0885	0.0510	-0.0160	8.55	12.65	0.995	0.0685	0.0141	-0.0145	9.15
14.15	0.740	0.181	0.151	-0.0823	11.55	12.75	0.853	0.132	0.0918	-0.0429	9.75	12.65	0.995	←Stall	-	-	9.15
						14.05	0.830	0.177	0.139	-0.0721	11.15	14.0	0.885	0.165	0.122	-0.0663	10.9
												15.3	0.880	0.193	0.150	-0.0808	12.2

Contd./

Table III (Contd.)

9% Wing

P = 11.4 Atmos. V = 49.0 FPS			ρV^2 = 62.6 lb./sq.ft. R = 2.20×10^6			P = 14.7 Atmos. V = 53.3 FPS			ρV^2 = 93.6 lb./sq.ft. R = 2.98×10^6			P = 18.5 Atmos. V = 57.9 FPS			ρV^2 = 138 lb./sq.ft. R = 4.05×10^6		
α	C_L	C_D	C_{D_o}	C_m	α_o	α	C_L	C_D	C_{D_o}	C_m	α_o	α	C_L	C_D	C_{D_o}	C_m	α_o
-2.2	-0.124	0.0090	0.0082	-0.0222	-1.75	-2.2	-0.125	0.0091	0.0082	-0.0223	-1.75	-2.2	-0.125	0.0093	0.0084	-0.0220	-1.75
-0.9	-0.026	0.0075	0.0075	-0.0211	-0.8	-0.9	-0.027	0.0078	0.0078	-0.0211	-0.8	-0.9	-0.028	0.0076	0.0076	-0.0209	-0.8
+0.35	+0.068	0.0068	0.0065	-0.0202	+0.1	+0.35	+0.068	0.0068	0.0066	-0.0202	+0.1	+0.35	+0.066	0.0073	0.0071	-0.0201	+0.1
1.6	0.165	0.0076	0.0061	-0.0192	1.0	1.6	0.163	0.0079	0.0064	-0.0193	1.0	1.6	0.160	0.0083	0.0069	-0.0191	1.05
2.85	0.256	0.0103	0.0067	-0.0184	1.95	2.85	0.253	0.0108	0.0073	-0.0184	1.95	2.85	0.256	0.0109	0.0073	-0.0180	1.95
5.25	0.435	0.0188	0.0084	-0.0175	3.7	4.05	0.351	-	-	-0.0174	2.85	4.05	0.349	-	-	-0.0176	2.8
7.75	0.629	0.0303	0.0085	-0.0161	5.55	5.25	0.442	0.0192	0.0085	-0.0172	3.7	5.25	0.444	0.0188	0.0080	-0.0169	3.7
9.0	0.727	0.0377	0.0087	-0.0153	6.45	7.75	0.631	0.0303	0.0083	-0.0167	5.55	7.75	0.635	0.0306	0.0084	-0.0164	5.55
10.15	0.818	0.0469	0.0101	-0.0157	7.25	10.15	0.827	0.0469	0.0094	-0.0163	7.25	10.2	0.820	0.0468	0.0097	-0.0163	7.3
12.65	0.986	0.0682	0.0141	-0.0165	9.15	12.65	1.00	0.0681	0.0130	-0.0173	9.15	12.65	1.008	0.0680	0.0120	-0.0168	9.1
13.9	1.085	0.0798	0.0148	-0.0162	10.1	15.15	1.185	0.0927	0.0156	-0.0169	11.0	13.9	1.095	0.0802	0.0144	-0.0172	10.05
15.15	1.165	0.0932	0.0186	-0.0164	11.05	16.35	1.26	0.1065	0.0193	-0.0170	11.9	15.2	1.18	0.0931	0.0162	-0.0176	11.0
16.35	1.238	0.107	0.0228	-0.0166	12.0	17.6	1.33	0.1225	0.0253	-0.0175	12.95	16.4	1.265	0.107	0.0191	-0.0179	11.95
17.6	1.315	0.122	0.0266	-0.0162	12.95	18.9	1.40	-	-	-0.0192	13.95	17.65	1.345	0.1215	0.0220	-0.0177	12.9
18.85	1.385	0.134	0.0283	-0.0166	14.0	19.7	1.435	←Stall	-	-	14.65	18.9	1.415	0.1355	0.0250	-0.0172	13.9
18.85	1.385	←Stall	-	-	14.0	20.5	0.87	0.299	0.258	-0.1042	17.45	20.15	1.475	←Stall	-	-	14.95
19.2	0.805	0.277	0.242	-0.1008	16.4							20.5	0.933	0.276	0.228	-0.0858	17.2
20.55	0.815	0.308	0.271	-0.1152	17.7							21.85	0.94	0.310	0.261	-0.1117	18.55

Contd./

Table III (Contd.)

9; ing

P = 22.8 Atmos. V = 63.9 FPS			ρV^2 = 216 lb./sq.ft. R = 5.76×10^6			P = 24.6 Atmos. V = 78.0 FPS			ρV^2 = 332 lb./sq. ft. R = 7.19×10^6		
α	C_L	C_D	C_{D_o}	C_m	α_o	α	C_L	C_D	C_{D_o}	C_m	α_o
-2.2	-0.122	0.0092	0.0084	-0.0221	-1.75	-2.2	-0.120	0.0093	0.0085	-0.0223	-1.75
-0.95	-0.026	0.0082	0.0082	-0.0214	-0.85	-0.95	-0.019	0.0078	0.0078	-0.0209	-0.85
+0.35	+0.071	0.0081	0.0078	-0.0200	+0.1	+0.35	+0.071	0.0078	0.0075	-0.0203	+0.1
1.6	0.162	-	-	-0.0192	1.05	1.6	0.164	0.0088	0.0073	-0.0192	1.05
2.85	0.259	0.0106	0.0069	-0.0182	1.95	2.85	0.258	0.0109	0.0072	-0.0183	1.95
5.3	0.445	-	-	-0.0167	3.75	4.05	0.347	-	-	-0.0176	2.85
7.75	0.634	0.0304	0.0082	-0.0158	5.55	5.3	0.451	0.0181	0.0070	-0.0168	3.7
10.2	0.822	0.0461	0.0089	-0.0150	7.3	7.8	0.640	0.0300	0.0074	-0.0158	5.5
12.7	1.008	0.0667	0.0110	-0.0156	9.15	10.25	0.828	0.0462	0.0083	-0.0153	7.35
13.95	1.098	0.0782	0.0119	-0.0162	10.1	12.8	1.012	0.0662	0.0100	-0.0154	9.2
15.2	1.180	0.0918	0.0151	-0.0159	11.05	14.0	1.100	0.0787	0.0124	-0.0156	10.1
16.4	1.268	0.1055	0.0170	-0.0156	11.95	15.25	1.185	0.0918	0.0144	-0.0155	11.1
17.7	1.345	0.1205	0.0208	-0.0168	12.95	16.5	1.27	0.1055	0.0165	-0.0155	12.05
18.95	1.420	0.136	0.0248	-0.0169	13.95	17.75	1.355	0.1275	0.0265	-0.0155	13.0
20.15	1.475	←Stall	-	-	14.95	19.05	1.415	-	-	-0.0154	15.3
20.45	0.999	0.257	0.202	-0.1004	16.95	19.4	1.430	←Stall	-	-	14.35
21.75	0.903	0.294	0.249	-0.1067	18.55	20.45	1.005	0.258	0.203	-0.1015	16.95

Table IV/

Table IV

11% Wing

P = 1.0 Atmos. V = 70.95 FPS			ρV^2 = 12.1 lb./sq.ft. R = 0.301×10^6		
α	C_L	C_D	C_{D_o}	C_m	α_o
-1.65	-0.057	0.0112	0.0110	-0.0278	-1.45
-0.6	+0.016	0.0107	0.0107	-0.0224	-0.65
+0.4	0.087	0.0114	0.0110	-0.0192	+0.1
1.45	0.159	0.0124	0.0110	-0.0166	0.9
2.5	0.232	0.0136	0.0106	-0.0133	1.7
5.55	0.450	0.0227	0.0115	-0.0080	3.95
8.65	0.638	0.0421	0.0195	-0.0024	6.4
9.7	0.690	0.0492	0.0228	+0.0003	7.25
10.75	0.750	0.0632	0.0320	0.0020	8.1
11.75	0.792	0.0879	0.0531	0.0010	8.95
12.85	0.785	0.1305	0.0964	-0.0206	10.05
13.95	0.746	0.167	0.136	-0.0486	11.3

P = 2.3 Atmos. V = 67.7 FPS			ρV^2 = 24.9 lb./sq.ft. R = 0.65×10^6		
α	C_L	C_D	C_{D_o}	C_m	α_o
-1.7	-0.053	0.0090	0.0088	-0.0279	-1.5
-0.6	+0.014	0.0073	0.0073	-0.0238	-0.65
+0.4	0.090	0.0076	0.0072	-0.0220	+0.1
1.45	0.166	0.0088	0.0073	-0.0207	0.85
2.5	0.249	0.0106	0.0072	-0.0193	1.6
5.6	0.446	0.0213	0.0103	-0.0089	4.0
8.7	0.645	0.0383	0.0152	-0.0033	6.4
9.75	0.706	0.0457	0.0180	-0.0017	7.25
10.8	0.770	0.0585	0.0246	-0.0005	8.05
11.85	0.810	0.0809	0.0444	+0.0006	8.95
12.95	0.817	0.119	0.0816	-0.0117	10.05
13.95	0.811	0.1525	0.116	-0.0318	11.05
15.0	0.785	0.184	0.150	-0.0538	12.2

P = 4.6 Atmos. V = 56.6 FTS			ρV^2 = 34.4 lb./sq.ft. R = 1.075×10^6		
α	C_L	C_D	C_{D_o}	C_m	α_o
-1.75	-0.051	0.0074	0.0072	-0.0277	-1.55
-0.65	+0.018	0.0052	0.0052	-0.0243	-0.7
+0.35	0.093	0.0058	0.0053	-0.0224	0
1.4	0.172	0.0066	0.0050	-0.0213	+0.8
2.5	0.251	0.0087	0.0052	-0.0200	1.6
5.55	0.458	0.0203	0.0086	-0.0122	3.95
8.7	0.664	0.0357	0.0113	-0.0066	6.35
10.75	0.798	0.0499	0.0146	-0.0041	7.9
11.8	0.824	0.0798	0.0422	-0.0005	8.9
12.9	0.824	0.116	0.0787	-0.0129	10.0
13.95	0.812	0.156	0.119	-0.0375	11.05
15.0	0.765	0.187	0.155	-0.0587	12.3
17.15	0.660	0.225	0.201	-0.0780	14.8

Contd./

Table IV (Contd.)

11% Wing

P = 9.58 Atmos., V = 53.0 FPS, ρV^2 = 62.5 lb./sq.ft., R = 2.08 × 10^6

α	C_L	C_D	C_{D_o}	C_m	$α_o$
-1.75	-0.066	0.0066	0.0064	-0.0269	-1.5
-0.7	+0.010	0.0053	0.0053	-0.0251	-0.75
+0.35	0.088	0.0052	0.0048	-0.0233	+0.05
1.4	0.172	0.0062	0.0046	-0.0222	0.8
2.5	0.248	0.0086	0.0052	-0.0209	1.6
5.6	0.468	0.0202	0.0080	-0.0140	3.95
8.75	0.697	0.0368	0.0098	-0.0111	6.25
11.85	0.904	0.0597	0.0143	-0.0090	8.65
14.95	1.105	0.0888	0.0208	-0.0066	11.05
17.05	1.22	0.1105	0.0281	-0.0054	12.7
18.1	1.265	0.123	0.0342	-0.0062	13.6
19.0	1.30	←Stall	-	-	14.45
19.25	0.73	0.262	0.232	-0.0862	16.65

P = 9.58 Atmos, V = 74.7 FPS, ρV^2 = 124.0 lb./sq.ft., R = 2.91 × 10^6

α	C_L	C_D	C_{D_o}	C_m	$α_o$
8.9	0.721	-	--	-0.0135	6.35
13.15	1.018	-	-	-0.0115	9.55
16.3	1.21	-	-	-0.0093	12.0
17.35	1.275	-	-	-0.0090	12.85
18.4	1.320	-	-	-0.0081	13.7
19.5	1.365	-	-	-0.0079	14.65
20.5	1.395	←Stall	-	-	15.6
20.3	0.832	-	-	-0.0901	17.35

P = 15.05 Atmos, V = 67.5 FPS, ρV^2 = 159 lb./sq.ft., R = 4.12 × 10^6

α	C_L	C_D	C_{D_o}	C_m	$α_o$
9.0	0.746	-	-	-0.0147	6.35
13.25	1.05	-	-	-0.0137	9.55
17.5	1.32	-	-	-0.0128	12.8
18.55	1.38	-	-	-0.0120	13.65
19.65	1.425	-	-	-0.0121	14.6
20.7	1.46	-	-	-0.0111	15.5
21.6	1.485	←Stall	-	-	16.4
21.6	0.945	-	-	-0.0889	18.2

P = 23.1 Atmos., V = 56.7 FPS, ρV^2 = 167.5 lb./sq.ft., R = 5.05 × 10^6

α	C_L	C_D	C_{D_o}	C_m	$α_o$
-1.8	-0.064	0.0076	0.0076	-0.0262	-1.55
-0.7	+0.020	0.0066	0.0066	-0.0247	-0.75
+0.35	0.101	0.0069	0.0063	-0.0232	-0.05
1.45	0.[illegible]83	0.0080	0.0061	-0.0220	+0.8
2.55	0.259	0.0108	0.0071	-0.0198	1.65
5.75	0.499	0.0218	0.0080	-0.0165	4.[illegible]
9.0	0.741	0.0393	0.0089	-0.0148	6.35
12.2	0.973	0.0634	0.0109	-0.0145	8.75
15.4	1.185	0.0943	0.0162	-0.0145	11.2
16.45	1.255	0.106	0.0182	-0.0147	12.0
17.5	1.32	0.117	0.0204	-0.0142	12.8
18.6	1.37	0.130	0.0257	-0.0137	13.7
19.7	1.425	0.1405	0.0275	-0.0132	14.65
20.75	1.46	0.154	0.0358	-0.0122	15.55
21.85	1.485	←Stall	-	-	15.65
21.6	0.985	0.273	0.219	-0.0792	1[illegible].1
22.5	0.925	0.313	0.265	-0.1040	19.2

Contd./

Table IV (Contd.)

11% Wing

P = 18.9 Atmos. V = 76.4 FPS			ρV² = 252 lb./sq.ft. R = 5.73 × 10⁶		
α	C_L	C_D	C_{D_o}	C_m	α_o
9.25	0.772	–	–	-0.0155	6.5
13.7	1.075	–	–	-0.0161	9.9
18.0	1.36	–	–	-0.0163	13.15
19.1	1.42	–	–	-0.0161	14.05
20.15	1.46	–	–	-0.0154	14.95
21.1	1.48	←Stall	–	–	15.9
20.8	0.99	–	–	-0.0649	17.3

P = 24.6 Atmos. V = 68.2 FPS			ρV^2 = 262 lb./sq.ft. R = 6.65×10^6		
α	C_L	C_D	C_{D_o}	C_m	α_o
-1.9	-0.083	0.0075	0.0070	-0.0245	-1.6
-0.75	+0.008	0.0072	0.0072	-0.0234	-0.8
+0.35	0.091	0.0075	0.0070	-0.0218	+0.5
1.5	0.179	0.0088	0.0070	-0.0204	0.85
2.6	0.264	0.0107	0.0068	-0.0188	1.65
5.9	0.516	0.0225	0.0078	-0.0160	4.05
9.3	0.768	0.0412	0.0086	-0.0148	6.6
11.5	0.932	0.0585	0.0105	-0.0148	8.2
13.7	1.085	0.0785	0.0132	-0.0152	9.85
15.85	1.225	0.1008	0.0175	-0.0155	11.5
16.95	1.305	0.1125	0.0181	-0.0158	12.3
18.05	1.355	0.125	0.0225	-0.0154	13.25
19.15	1.41	0.136	0.0258	-0.0143	14.15
20.25	–	0.158	0.0899	-0.0096	–
20.7	1.465	←Stall	–	–	15.55
20.75	1.08	0.253	0.187	-0.0776	16.9

P = 24.0 Atmos. V = 82.2 FPS			ρV^2 = 366 lb./sq.ft. R = 7.64×10^6		
α	C_L	C_D	C_{D_o}	C_m	α_o
-2.0	-0.088	0.0078	0.0074	-0.0246	-1.7
-0.8	+0.002	0.0070	0.0070	-0.0231	-0.85
+0.35	0.094	0.0072	0.0068	-0.0219	0
1.55	0.186	0.0088	0.0069	-0.0207	+0.9
2.65	0.273	0.0112	0.0071	-0.0188	1.7
6.15	0.543	0.0237	0.0073	-0.0161	4.2
9.6	0.801	0.0447	0.0091	-0.0151	6.75
13.0	1.05	0.0732	0.0118	-0.0164	9.3
16.4	1.28	0.108	0.0176	-0.0177	11.85
17.5	1.345	0.120	0.0191	-0.0177	12.7
18.6	1.40	0.133	0.0239	-0.0171	13.65
19.75	1.44	0.161	0.0464	-0.0155	14.65
20.25	1.455	←Stall	–	–	15.15
20.15	1.14	0.234	0.162	-0.0652	16.1
21.05	1.04	0.267	0.207	-0.0755	17.35

JW

APPENDIX

June, 1952

Summary

Since the original report was written the models have been examined qualitatively by a visual method using tufts attached to the upper surface.

It was found that these tufts could be placed almost anywhere on the surface of the 9% aerofoil without appreciable effect on the flow conditions, but that the 11% was sensitive to their presence anywhere on the forward half. Nevertheless, by combining balance measurements with tufting in order to obtain the optimum tuft arrangement, good correlation was obtained between the flow pattern development and the true C_L — α curves.

At high Reynolds numbers the 9% section stalls sharply by separation from near the leading edge. This is also true of the 11% except that by the time it occurs, turbulent separation has spread well forward from the rear. Below the critical R breakdown of the flow pattern is associated with an early development of a nose bubble separation.

Out of a number of other profiles having a similar critical scale effect on $C_{L}max$, one has been selected for comparison and contrast. It is demonstrated that in the case of these three aerofoils (two cambered and each of 8 inch chord and one symmetrical with a chord of 12 inches) the stall occurs when the forward parts (which are similar in form and linear dimensions) of the upper surfaces reach a certain attitude with respect to the wind. This may indicate that separation in the peak suction region depends to some extent on the size as well as the shape of the nose profile.

Arrangements of Tufts

Tufts on a model in the Compressed Air Tunnel can be viewed through one of the small spyholes after reflection in a mirror and Fig. 4 shows their arrangement on the Vickers wings. They consisted of thin wool streamers affixed to the surface by Araldite 101 and it will be noticed that they were staggered so as to keep the rearward tufts clear of any wake produced by those nearer the leading edge.

In addition to attempting to investigate the development of the stalled conditions a few experiments were carried out to examine whether the tufts themselves were causing an appreciable interference with the flow pattern. For that reason the lay-out in each case included originally a set parallel to, and half an inch from, the leading edge.

Development of the Stalled Conditions

In spite of the interference caused by the tufts on the 11% wing which will be discussed later, it is thought that the flow changes can be fairly well defined as follows:-

Below the Critical R .- In each case a separation region (nose bubble) forms along the centre part of the leading edge at an incidence (10° for the 9% and 11° for the 11%), not far short of the incidence of maximum lift, where the slope of the C_L — α curve begins to decrease very appreciably. On the 9% the boundary layer behind this is turbulent, but on the 11% only a narrow strip along the trailing edge is subject to unsteadiness. In the early stages reattachment on the latter section does not appear to be associated with a breakdown of the steady flow.

/As

As the lift coefficient passes through its maximum with increasing incidence the centre two thirds of the wing becomes stalled. In the first case the separation region spreads rearwards and sideways from the nose bubble, and in the second it spreads simultaneously rearwards from the leading edge and forwards from the trailing edge.

The C_L — α curves below the critical R have rounded t ps corresponding to the comparatively gradual stall. There is, however, no indication to be associated with the pronounced loss of slope for the 11% section above a value of C_L of about 0.25 at these Reynolds numbers.

<u>Above the Critical R</u>.- Above the critical Reynolds number the first indication is an unsteadiness at the trailing edge. The 9% wing later stalls suddenly by separation from the leading edge but on the 11%, turbulent separation first develops at the trailing edge and spreads well forward before a similar breakdown occurs at the leading edge. This fits in with the shape of the C_L — α curve which bends over only very slightly for the 9% but much more so for the 11% (Fig. 3).

On the latter the stall is a race between a sharp leading edge stall and a forward movement of the rear separation. Presumably the peak suction and the rear separation influence one another. On the 9%, however, it appears that as regards profile outline the stall is determined entirely by the nose shape and that it might be possible to improve $C_{L}max.$ quite appreciably by increasing the camber.

<u>In the Critical Range of R</u>.- The behaviour in this range is naturally more indefinite. Generally an incipient unsteadiness is set up at the trailing edge at moderate angles of incidence followed later by a very sharp stall, but occasionally at an intermediate stage, a small separation region develops in the centre of the span and at about 0.2c from the leading edge.

<u>General</u>.- It might be anticipated that the greater slope of the C_L — α curves of the 9% aerofoil at fairly high values of C_L compared with that for $C_L = 0$ would indicate the presence of a nose bubble at low incidence even at high Reynolds numbers. This, however, could not be detected. In the $C_m = C_L$ curves there were no significant peculiarities which could be linked up with the tuft indications below the stall.

<u>Interference Effect of Tufts</u>

In order to illustrate the severe interference that can sometimes arise when an aerofoil is tufted, or perhaps over-tufted, angles of stalling incidence are plotted in Fig. 4 under various conditions, in relation to the values found previously during the balance measurements. They refer, of course, only to the range of Reynolds number where the stall is fairly sharp and although the new values are not very precise the errors are not important.

The curves show that the effect of the presence of the tufts on the 9% wing is quite small even when the leading edge tufts are in place. It may be expected therefore that the flow picture obtained will be a f rly good representation of the development of stalled conditions.

/On

On the 11% wing on the other hand the interference caused by the tufts is quite definite and seems to be independent of whether those at the leading edge are present or not. At the highest Reynolds numbers the stall of the tufted 11% model was always of a very spasmodic nature and hardly consistent with the sharp stall obtained during the balance measurements. It appears that the separation at the leading edge is in this case much affected by slight changes in the turbulent separation region further back.

For comparison the corresponding results for what is called the HSA5 B section (symmetrical) are also included in Fig. 4. The ordinates of this section may be defined as being equal to those of the AN510-009 plus one third of the difference between this and the HSA5. The chord of this aerofoil was 12 inches but the first line of tufts was still half an inch from the leading edge. These results show that this line of tufts vitiated the flow pattern completely while the others had very little influence except possibly at high values of R. This section stalls sharply from near the leading edge without preliminary disturbance anywhere in the boundary layer.

Limitations of Tufting Experiments

It is clear that any investigation of flow pattern near the stall by a technique involving the use of streamers must be undertaken with an acute awareness of its limitations. Tufts near the peak suction positions of an aerofoil are very liable to upset the flow completely but are sometimes quite safe. On the other hand, careful tufting of the rear half of the upper surface is usually safe but on some aerofoil sections the flow near the nose appears to be particularly sensitive to what is happening over the rear half.

Unless the major changes of flow pattern can be correlated with definite changes of lift or moment characteristics the indications must be accepted with some reserve.

The best technique is to approach the surface with a streamer attached to the end of a probe but unfortunately this is often a slow and inconvenient process.

Comparison of Profile Shapes

The similarities and differences have also been considered from another angle. The symmetrical HSA5 B aerofoil was originally selected out of a number of aerofoils having a critical rise in $C_L max$ with R first because this critical occurred at nearly the same value as for the Vickers wings and secondly because the theoretical nose shape was somewhat similar. The actual nose profile was, however, later measured up and found to be a little blunter than is indicated in the derivation given above, i.e. the section was very slightly truncated at the leading edge. The three profiles (HSA5 B as measured) up to one inch from the leading edge are drawn in Fig. 5.

It was found that they could be superimposed as regards the upper surface for a distance of 0.8 inch from the leading edge and it was realized that the stall took place when this part of the three surfaces reached approximately the same attitude with respect to the wind (cf. Fig. 4).

/The

The flow on the HSA5 B aerofoil at $C_L$max separates sharply from near the leading edge with no preliminary disturbance anywhere in the boundary layer. The conclusion is that in each case the breakdown is primarily due to the suction peak conditions and that it may depend not only on the nose shape but, remembering that the HSA5 B is a 12 inch chord aerofoil, also on the actual linear dimensions.

Conclusions

It has been found that tufts can be placed almost anywhere on the surface of the 9% aerofoil without appreciable effect on the flow conditions but that the 11% is sensitive to their presence anywhere in the forward half. Interference effects of surface tufts are so unpredictable that other tests must be applied in order to find their optimum arrangement.

At high Reynolds numbers the 9% section stalls sharply by separation from near the leading edge. This is also true of the 11% except that by the time this occurs turbulent separation has spread well forward from the rear. It appears that in respect of the former it might be possible to improve $C_L$max appreciably by increasing the camber.

Below the critical R breakdown of the flow pattern is associated with an early development of a nose bubble separation.

Comparing the 8 inch chord cambered Vickers' wings with one another and with the 12 inch symmetrical HSA5.B, all of which are similar as regards form and dimensions for a distance of 0.8 inch along the upper surface from the leading edge, it is found that stalling occurs when these portions of the upper surface reach a certain attitude with respect to the wind. It may be an indication that breakdown of the flow in this region depends not only on the profile shape near the leading edge but also on the actual linear dimensions.

Aerofoil Profile 9% T/c

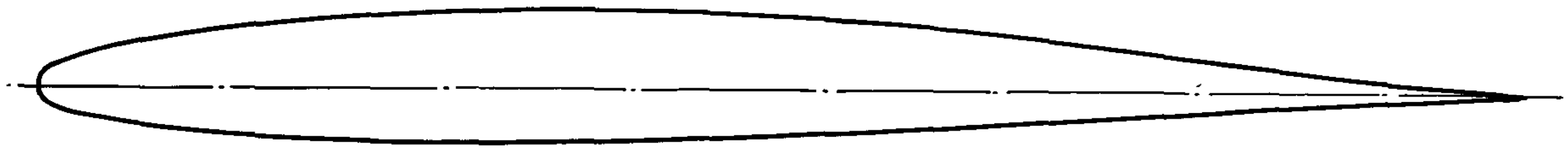

Aerofoil Profile 11% T/c

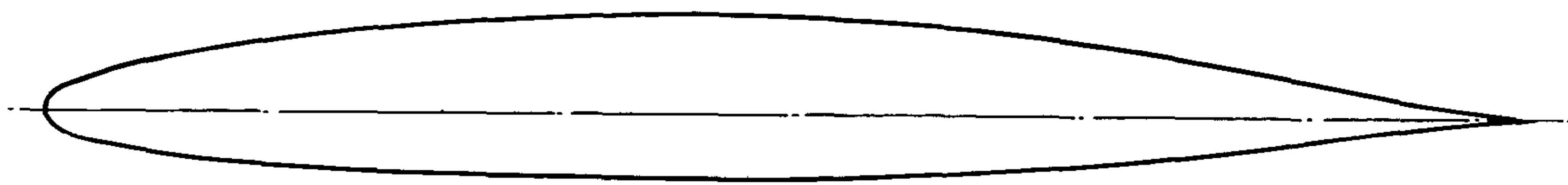

Vickers 9% & 11% Wings

13,787
FIG 1

EEM

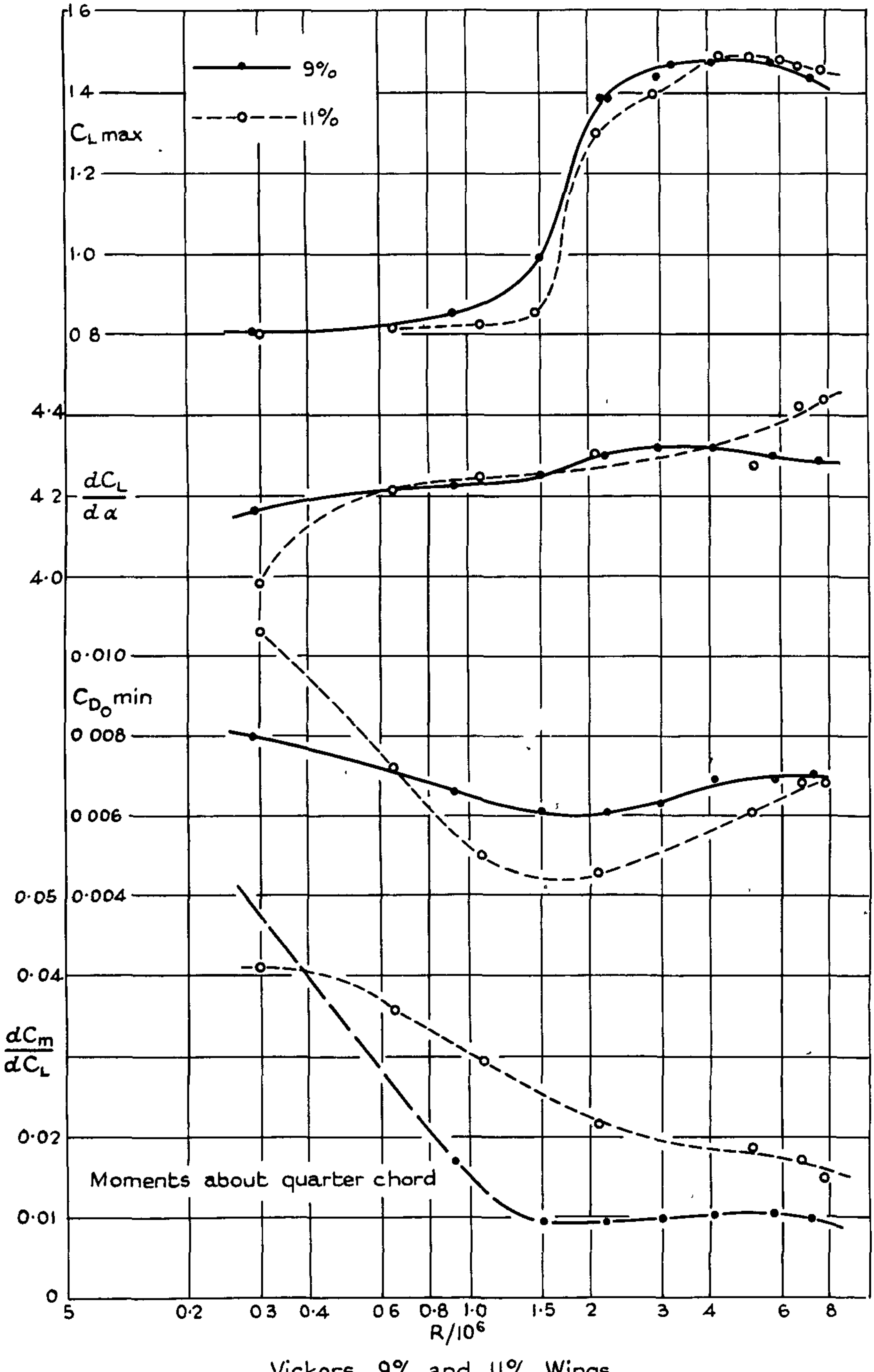

Vickers 9% and 11% Wings.

EEM

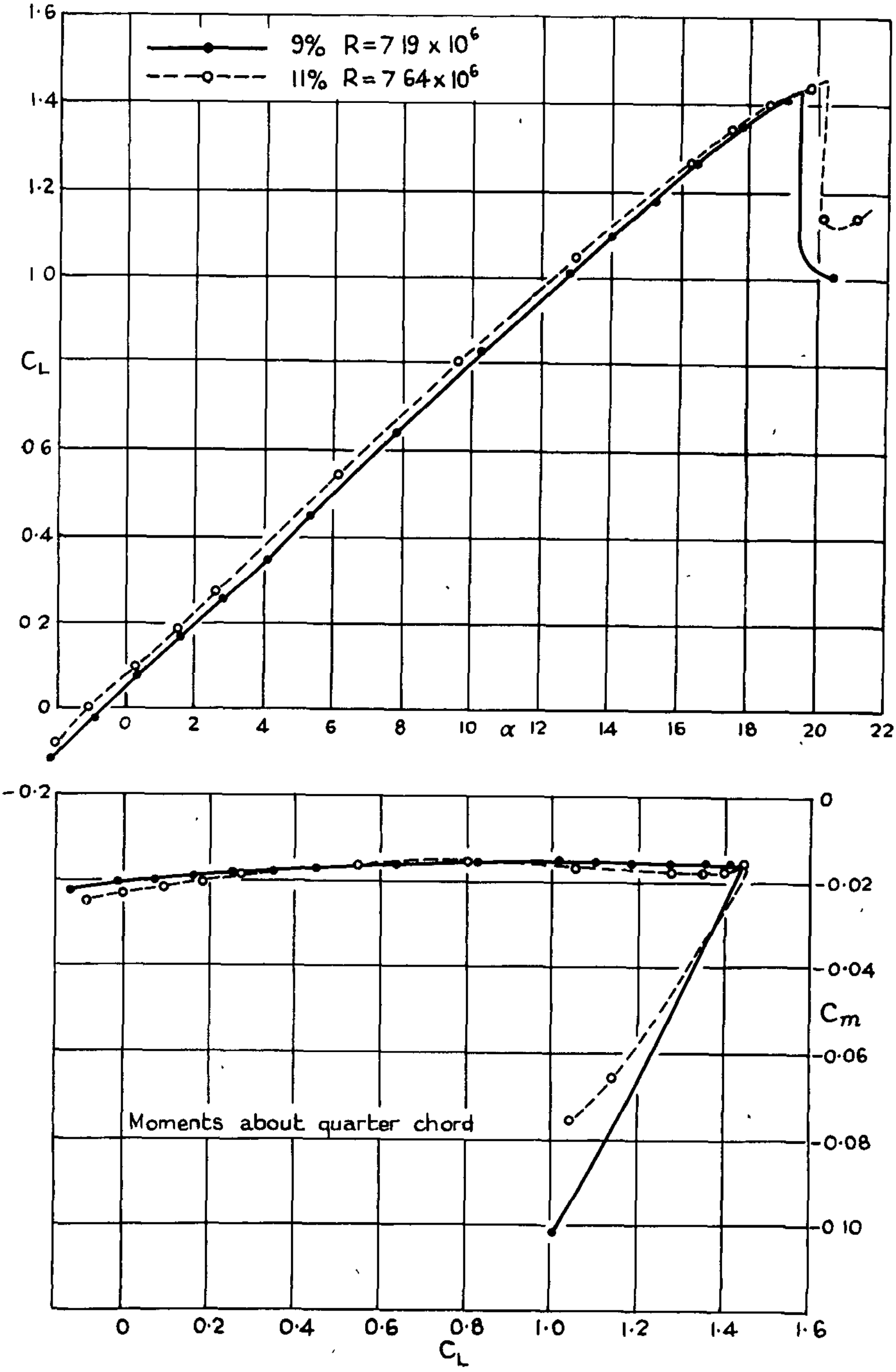

Vickers 9% and 11% Wings.

EEM

FIG 4

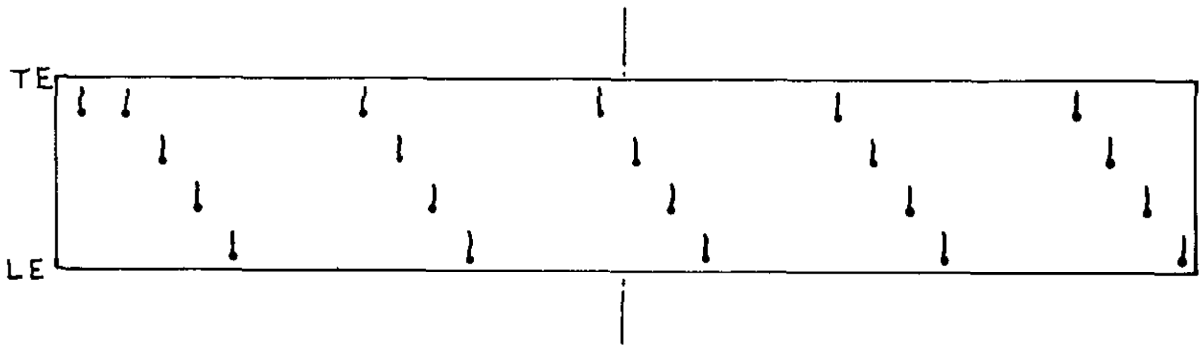

Arrangement of Tufts as veiwed in Mirror
Wing 48" x 8"

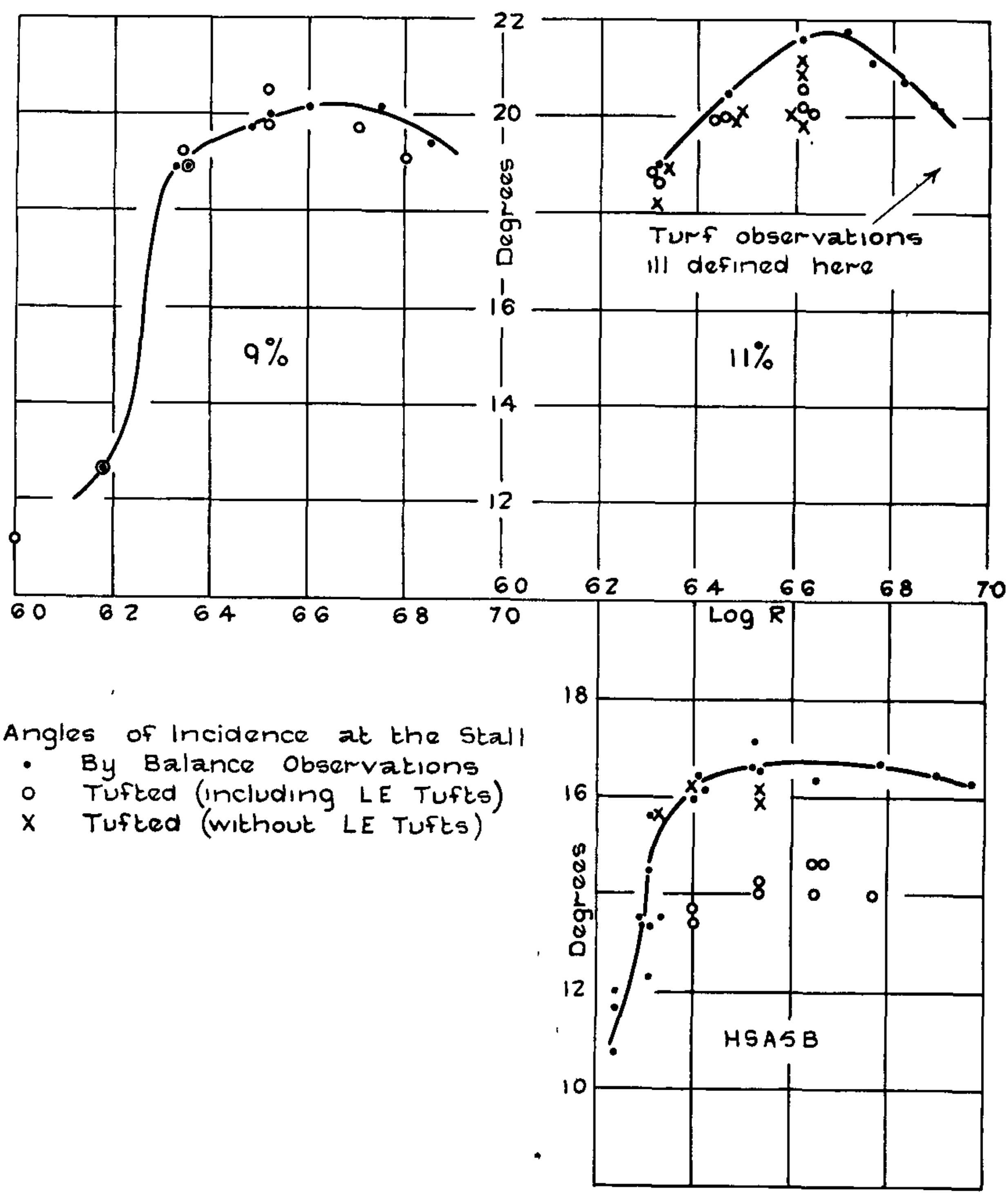

Angles of Incidence at the Stall
• By Balance Observations
o Tufted (including LE Tufts)
X Tufted (without LE Tufts)

Vickers 9% and 11% Wings

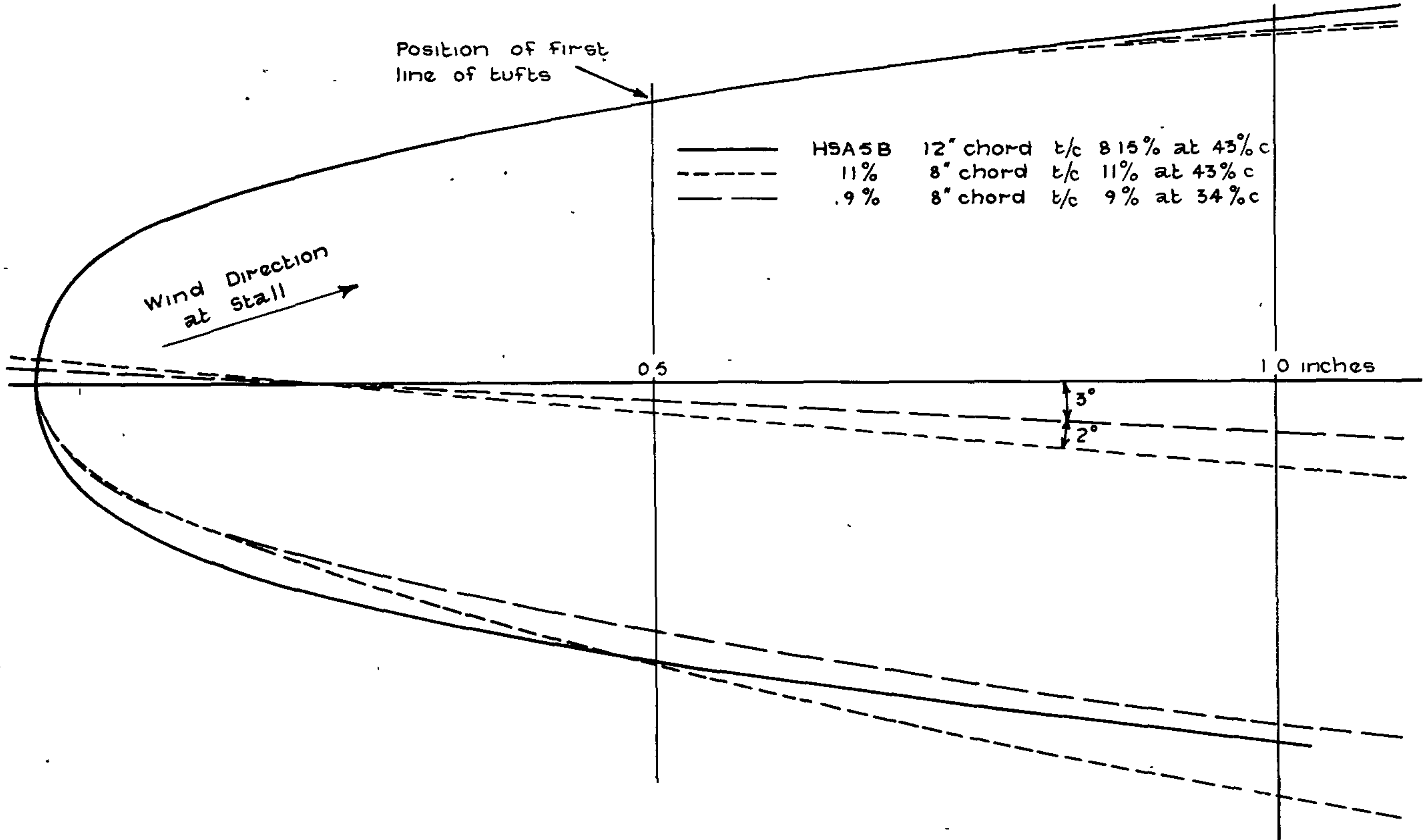

Vickers 9% and 11% and HSA5B

FIG. 5

C.P. No. 92
(13,787)

A.R.C. Technical Report

PRINTED AND PUBLISHED BY HER MAJESTY'S STATIONERY OFFICE

To be purchased from

York House, Kingsway, LONDON, W.C.2 423 Oxford Street, LONDON, W.1

P.O. Box 569, LONDON, S.E.1

13a Castle Street, EDINBURGH, 2 1 St. Andrew's Crescent, CARDIFF

39 King Street, MANCHESTER, 2 Tower Lane, BRISTOL, 1

2 Edmund Street, BIRMINGHAM, 3 80 Chichester Street, BELFAST

or from any Bookseller

1952

Price 4s 0d net

PRINTED IN GREAT BRITAIN

S.O. Code No. 23-9006-92